Water Science & Technology

IWA PUBLISHING

Water Science & Technology Vol 89 No 7, 1630 doi: 10.2166/wst.2024.080

Response surface optimization of sludge dewatering process: synergistic enhancement by ultrasonic, chitosan and sludge-based biochar

Yahong Yang[a,b,*], Xingfeng Yang[a,c], Yirong Chen[a,b], Xiaowei Li[c], Qiyong Yang[d], Yangying Li[a,b], Pengjing Ma[a,b], Huining Zhang[a] and Shenghui Xu[a]

[a] School of Civil Engineering, Lanzhou University of Technology, Lanzhou, Gansu 730050, China
[b] Wenzhou Engineering Institute of Pump & Value, Lanzhou University of Technology, Wenzhou, Zhejiang 325105, China
[c] School of Environmental and Chemical Engineering, Organic Compound Pollution Control Engineering, Ministry of Education, Shanghai University, Shanghai 200444, China
[d] College of Resources & Environment, Jiujiang University, Jiujiang, Jiangxi 332005, China
*Corresponding author. E-mail: 76426321@qq.com

ABSTRACT

Due to the colloidal stability, the high compressibility and the high hydration of extracellular polymeric substances (EPS), it is difficult to efficiently dehydrate sludge. In order to enhance sludge dewatering, the process of ultrasonic (US) cracking, chitosan (CTS) re-flocculation and sludge-based biochar (SBB) skeleton adsorption of water-holding substances to regulate sludge dewaterability was proposed. Based on the response surface method, the prediction model of the specific resistance to filtration (SRF) and sludge cake moisture content (MC) was established. The US cracking time and the dosage of CTS and SBB were optimized. The results showed that the optimal parameters of the three were 5.08 s, 10.1 mg/g dry solids (DS) and 0.477 g/g DS, respectively. Meantime, the SRF and MC were 5.4125×10^{11} m/kg and 76.8123%, which significantly improved the sludge dewaterability. According to the variance analysis, it is found that the fitting degree of SRF and MC model is good, which also confirms that there is significant interaction and synergy between US, CTS and SBB, and the contribution of CTS and SBB is greater. Moreover, the process significantly improves the sludge's calorific value and makes its combustion more durable.

Key words: calorific value, response surface method (RSM), sludge-based biochar, sludge dewaterability, thermogravimetric analysis

HIGHLIGHTS

- Ultrasonic (US) cracking, chitosan (CTS) flocculation and sludge-based biochar (SBB) adsorption of water-holding substances synergistically enhance sludge dewaterability.
- Response surface methodology (RSM) was used to optimize the US time and the dosage of CTS and SBB.
- Established predictive models for the specific resistance to filtration and sludge cake moisture content.

GRAPHICAL ABSTRACT

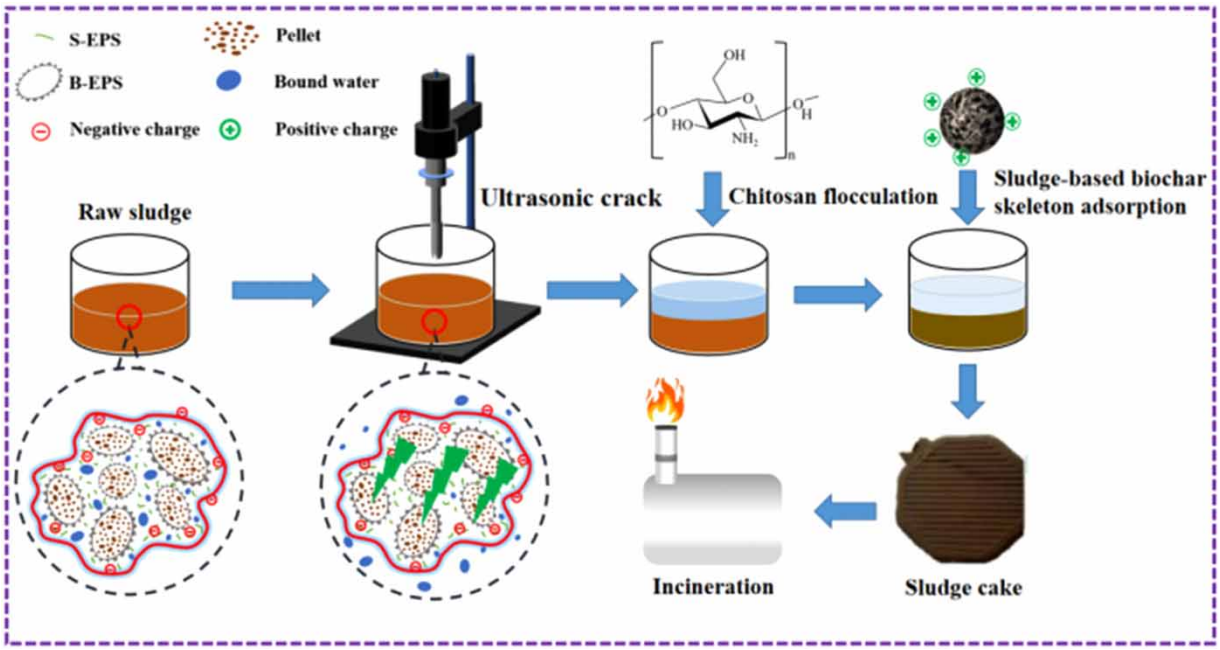

ABBREVIATIONS

WWTPs	wastewater treatment plants
EPS	extracellular polymeric substance
S-EPS	soluble EPS
LB-EPS	loosely bound EPS
TB-EPS	tightly bound EPS
PN	proteins
PS	polysaccharides
US	ultrasonic
CTS	chitosan
SBB	sludge-based biochar
RSM	RESPONSE surface method
SRF	specific resistance to filtration
MC	moisture content
BBD	Box–Behnken design method
CCD	central composite design method
ANOVA	analysis of variance
TG-DTG	thermogravimetric analysis
A^2/O	anaerobic–anoxic–oxic

1. INTRODUCTION

The amount of sewage in wastewater treatment plants (WWTPs) is increasing, and the excess sludge generated by biological treatment is also increasing (Huang *et al.* 2020a, 2020b). According to statistics, 40 million tons of excess sludge with 80% water content are produced annually in China (Wang *et al.* 2020). Biological treatment of wastewater will inevitably produce massive excess sludge. The moisture content (MC) of these sludges is generally 95–99%, and they contain a large number of dangerous substances such as parasite eggs, pathogenic bacteria and refractory heavy metals. If they are not effectively treated, they will have a negative impact on the ecological environment and human activities (Wu *et al.* 2020a; Cao *et al.* 2021). Therefore, the large amount of sludge determines that sludge treatment should account for a large proportion in the secondary pollution control of WWTPs, in which sludge dewatering is a common technical unit for sludge treatment (Chen *et al.* 2015).

Sludge is a kind of biological solid, and its floc structure contains huge amounts of extracellular polymeric substance (EPS) and bound water (Mowla *et al.* 2013). EPS has strong hydrophilicity, mainly including proteins (PN) and polysaccharides (PS) with strong hydrophilicity and viscosity (Zhang *et al.* 2015). EPS is distributed around the bacterial cell wall. The cell wall with the semi-rigid structure of bacterial cells plays a role in protecting microbial cells. General mechanical dehydration cannot destroy the bacterial micelle structure of sludge, resulting in some difficulties in sludge dehydration. In recent years, researchers have explored a variety of methods for sludge cracking, all of which destroy cells by destroying the floc structure and cell wall of sludge, promote the release of EPS-bound water and other substances and thus improve the dewaterability of sludge. Sludge cracking technology includes chemical methods, physical methods and biological methods. The chemical method usually uses the oxidation method to crack sludge (Zhou *et al.* 2014; Lin *et al.* 2022). The chemical method typically employs oxidation techniques to break down sludge, using substances like hydrogen peroxide (Lu *et al.* 2001), persulfate (Fan *et al.* 2021), permanganate (Zhang *et al.* 2018) and ozone (Ge *et al.* 2020). Chemical agents need to be added to react with sludge, which is easy to cause secondary pollution; Physical methods are generally freeze-thaw or heat treatment (Gao 2011; Feng *et al.* 2014), but their energy consumption is high; biological method generally uses bioleaching acidification to break the sludge (Wong *et al.* 2015), with good effect, but it takes a long time. Ultrasonic (US) technology is widely used in the field of sludge treatment. Its mechanical effect, thermal effect and free radical effect can deconstruct the sludge micelles, decompose cells, promote the dissolution and dissolution of intracellular substances and reduce the size of sludge particles (Zielewicz 2016; Xu *et al.* 2019). Yu *et al.* (2008) reported that US treatment of sludge can promote the transfer of proteins, PS and enzymes from the inner layer EPS of sludge to the outer layer EPS, thereby improving the dewatering performance and digestion performance of sludge.

Part of the water molecules in the sludge are closely combined with the solid phase and uniformly distributed in the colloidal system as a dispersed phase. Moreover, the particle size of the sludge colloid is small and the specific surface area is large, so it is easy to physically adsorb the water molecules; in addition, some functional groups on the surface of sludge colloid have extremely strong hydrophilicity, which makes it difficult for sludge to effectively dehydrate (Chen *et al.* 2015; Ge *et al.* 2019). Adding flocculant can make the sludge colloid destabilize and aggregate, increase the particle size of the sludge, reduce the hydrophilicity of the colloid and strengthen the solid–liquid separation. Long-term use of conventional chemical flocculants such as ferric chloride ($FeCl_3$), poly aluminum chloride (PAC) and polyacrylamide (PAM) may lead to secondary environmental pollution problems such as heavy metal enrichment in sludge (Bala Subramanian *et al.* 2010; Guo & Chen 2017). Natural polymer flocculants are favored by researchers because of their wide source, non-toxic and easy biodegradation. Chitosan (CTS) is a new type of green flocculant. Its molecule contains amino ($-NH_2$), hydroxymethyl ($-CH_2OH$) and hydroxyl (-OH) groups (Shi *et al.* 2019). When $-NH_2$ obtains proton (H^+), the long molecular chain of CTS carries cationic groups, which makes it have the characteristics of cationic flocculant. Zhang *et al.* (2019) found that after CTS conditioning, the water content of the filter cake of the sludge decreased from 85.9 to 83.0%, the SV_{30} decreased to about 1/2, and the sludge volume decreased to 82.9%.

The high compressibility of the sludge makes it easy to deform under the action of external forces, so the filter channel in the filter cake will be blocked, which hinders the penetration of water (Agarwal *et al.* 2005). Therefore, the compressibility of the sludge becomes the key factor to determine the final dehydration performance of the sludge. It has been found that by adding skeleton particles with rigid structure or high porosity, a hard grid structure can be built in the sludge system, which improves the mechanical strength of the sludge, so that it can maintain the porous and permeable structure under the high pressure or strong shear force of the dewatering machine, thereby improving the removal efficiency of water in the sludge (Qi *et al.* 2011; Masihi & Badalians Gholikandi 2021). Previous results indicate that pyrolyzing dewatered sludge to produce sludge-based biochar (SBB) effectively reduces the compressibility of the sludge (Yang *et al.* 2022a). Not only that, the study also found that the abundant cationic functional groups on the surface of SBB make it have the effect of promoting flocculation, can adsorb proteins and PS in EPS, promote the dissolution of internal EPS and effectively weaken the water retention capacity of sludge flocs. As a new skeleton particle, SBB is a green and sustainable new idea applied to sludge dewatering, which greatly promotes the development of sludge closed-loop disposal routes.

Based on the above description, we propose a new sludge conditioning process: SBB framework construction and adsorption of water-holding substances coupled with US cracking and CTS re-flocculation for sludge conditioning, to solve the problem of sludge dehydration difficulty. Through the previous research, it was found that this process can greatly enhance sludge dewaterability (Yang *et al.* 2022b). Among them, the cracking time of US and the dosage of CTS and SBB are

considered to be important process parameters in the conditioning process, which need to be further optimized to obtain a better conditioning effect. The response surface method (RSM) is an experimental optimization method based on mathematical statistics. It can establish the functional model relationship between independent variables and response variables by designing fewer test groups, analyze the interaction relationship between influencing factors and determine the optimal combination of each factor level (Mohajeri *et al.* 2010). In addition, sludge reduction and harmlessness can be quickly realized through incineration, especially in the current period of the novel coronavirus epidemic, the sludge of WWTPs has the risk of virus occurrence, and incineration treatment can eliminate this risk (Ducoli *et al.* 2021). The incineration ash obtained from the combustion of sludge can be used to produce building materials or concrete aggregates, and the recovery of phosphorus from the incineration ash has also received more and more attention (Liang *et al.* 2021).

The purpose of this study is to use RSM to design three factors and three levels of optimization test, to obtain the optimal condition parameters of US + CTS + SBB combined conditioning and to analyze the influence of the conditioning process on sludge EPS and surface functional groups, so as to analyze the sludge dehydration mechanism. The results of the study provide a basis for the future practical operation of the combined process. In addition, this study also discusses the influence of sludge conditioning on sludge incineration disposal by analyzing the changes in calorific value and thermogravimetric of sludge cake before and after sludge conditioning, which is intended to provide theoretical reference for subsequent sludge incineration disposal.

2. MATERIALS AND METHODS

2.1. Experimental materials

Aqueous sludge samples used in this study were taken from the sludge regulating tank of a WWTP in Lanzhou City, China. The treatment scale of the plant was 200,000 m^3/day and the treatment process was anaerobic–anoxic–oxic (A^2/O). The generated residual sludge was conditioned by adding PAM, and the conditioned sludge was dewatered by a centrifugal dehydrator to obtain a mud cake with an MC of about 80%. The water-bearing sludge samples were stored in a refrigerator at 4 °C and can only be stored for 3 days. The basic parameters of water-bearing sludge are shown in Table S1.

The ultrasonic equipment used in this study was purchased from Fuzhou Desen Precision Industry Co., Ltd Chitosan (degree of deacetylation: 80–95%) was purchased from Sinopharm Chemical Reagent Co., Ltd CTS solution was prepared with 1% HAc solution. HAc was purchased from Tianjin Kemiou Chemical Reagent Co., Ltd SBB was prepared by pyrolysis of dehydrated sludge, in which $ZnCl_2$ pre-activation was used in the activation stage, and $ZnCl_2$ was purchased from Shanghai Macklin Biochemical Co., Ltd Specific preparation methods was referred to Velghe *et al.* (2012). 80–180 μm SBB was screened out by 80 mesh and 180 mesh sieves.

2.2. Sludge conditioning experiment

The sludge conditioning experiment was carried out with 100 mL of sludge. The order of combined conditioning was as follows: firstly, the sludge was broken by US, and then CTS and SBB were added in turn. The frequency of US was 20 kHz, and the sound intensity was 1,000 W/m^2. The concentration of CTS was 0.5 g/L. After adding CTS, the stirrer was used to quickly stir for 30 s at a speed of 150 r/min and then slowly stir for 5 min at a speed of 50 r/min. After adding SBB, the stirrer was used to quickly stir for 1 min at a speed of 200 r/min and then slowly stir for 5 min at a speed of 50 r/min. The sludge after conditioning was subjected to subsequent sludge dewaterability tests. Each experiment was performed at least twice and averaged.

2.3. Analysis method

The test method of the specific resistance to filtration (SRF) of sludge was referenced from a previously reported study (Yang *et al.* 2022a). The sludge filter cake MC was measured by gravimetric method (Chen *et al.* 2010). Sludge EPS is composed of soluble EPS (S-EPS) and fixed-bound EPS (B-EPS). The latter presents a dynamic two-component structure, consisting of loosely bound EPS (LB-EPS) and tightly bound EPS (TB-EPS). EPS of each layer was extracted by an improved thermal extraction method (Chen *et al.* 2015). After the EPS extraction of each layer, the protein and polysaccharide contents of the samples were determined, respectively. The anthrone sulfuric acid colorimetry was used for PS and the protein kit method was used for PN (Yang *et al.* 2022b). After 24 h of vacuum drying, the sludge samples were ground, and the functional groups on the surface of the sludge were analyzed and determined by FTIR spectrometer (Nicolet is 50). The scanning

wavelength is 4,000–500 cm^{-1}. The low calorific value of the sludge cake was measured by an oxygen bomb calorimeter (SDC712). A thermogravimetric analyzer (STA449-F5) was used to conduct the thermogravimetric test on the sludge cake.

2.4. RSM analysis method

RSM was used to optimize the combined process conditions of sludge dewaterability, and Design-Expert 12 software was used for processing and analysis. The experimental design methods of the response surface quadratic model are generally the following three kinds: central composite design method (CCD), 3^k full factor method and Box–Behnken design method (BBD). In this study, the BBD experimental design method was used. The BBD has the following advantages (Ferreira *et al.* 2007; Zolgharnein *et al.* 2013): (1) it is suitable for experiments with less influence factors (three to five influence factors, three levels). (2) The test times are generally 15–62 times. When the number of influence factors is equal, the BBD method is less than the CCD. (3) The nonlinear relationship of influence factors can be obtained; (4) applicable to tests where all factors are measured; (5) can test the model fitting degree is insufficient. According to the test results, a second-order polynomial fitting model of response variables can be constructed, as shown in the following equation.

$$Y = \beta_0 + \sum_{i=1}^{m} \beta_i x_i + \sum_{i=1}^{m} \beta_{ii} x_i x_i + \sum \sum_{i<j} \beta_{ij} x_i x_j + \varepsilon \quad (1)$$

Y represents the response value, β_0, β_i, β_{ii}, β_{ij} represent the regression coefficient of the model. X_i, X_j represent input encoding variables; ε denotes the observation error.

In order to determine the optimal conditions for conditioning sludge dewaterability by US + CTS + SBB combined process, three important factors, namely US cracking time (X_1), CTS dosage (X_2) and SBB dosage (X_3), were selected as independent variables, and SRF and MC were, respectively, taken as the response values Y_{SRF} and Y_{MC} of sludge dewaterability. The coupling optimization experiment of three factors and three levels was designed by using Design-Expert 12 software and the BBD method.

3. RESULTS AND DISCUSSION

3.1. Level setting of influencing factors and RSM test design

The coded values −1, 0 and +1 are used to represent the low, medium and high test levels of each factor. Based on the previous experimental results (Yang *et al.* 2022b), a reasonable condition range value is selected as the respective coding level. The specific factor range and level setting are shown in Table 1. Thus, 17 groups of multifactor coupling tests were designed, and experiments were carried out according to these 17 groups of test settings. The results are shown in Table 2. The experimental ranges of response values Y_{SRF} and Y_{MC} were 5.05–7.53 × 10^{11} m/kg and 76.12–78.76%, respectively, and the predicted ranges were 5.36–7.60 × 10^{11} m/kg and 76.31–78.62%, respectively. Numerically, the predicted values are in good agreement with the experimental values.

3.2. Model construction and ANOVA

Using Design-Expert 12 software, the relationship between response values (Y_{SRF}, Y_{MC}) and influencing factors was fitted by ternary quadratic regression equation, and the functional relationship model between sludge dewatering performance (SRF,

Table 1 | Scope and level setting of variables

Variables	Code Coded values	Scopes and levels −1	0	1
US time (s)	X_1	4	5	6
CTS dosage (mg/g DS)	X_2	8	10	12
SBB dosage (g/g DS)	X_3	0.4	0.5	0.6

Table 2 | RSM[a] test design and results

	Factors			SRF (10^{11} m/kg)		MC (%)	
Run no.	X_1	X_1	X_3	Actual	Predicted	Actual	Predicted
1	6	12	0.5	6.22	6.19	77.61	77.72
2	5	8	0.4	7.53	7.41	77.73	77.89
3	4	10	0.6	6.01	5.89	77.50	77.55
4	6	8	0.5	7.49	7.51	78.48	78.38
5	4	10	0.4	6.20	6.30	77.63	77.58
6	5	10	0.5	5.05	5.36	76.12	76.31
7	5	10	0.5	5.50	5.36	76.39	76.31
8	4	8	0.5	6.20	6.24	77.62	77.52
9	5	8	0.6	6.65	6.73	77.89	77.94
10	5	12	0.4	6.28	6.20	77.73	77.68
11	5	12	0.6	7.47	7.60	78.76	78.60
12	6	10	0.6	6.88	6.79	77.98	78.04
13	5	10	0.5	5.45	5.36	76.42	76.31
14	4	12	0.5	7.23	7.21	78.52	78.62
15	5	10	0.5	5.45	5.36	76.34	76.31
16	5	10	0.5	5.32	5.36	76.31	76.31
17	6	10	0.4	5.55	5.66	77.10	77.05

[a]Response surface method.

MC) and conditioning conditions was constructed. The model equations are as follows:

$$\begin{aligned} Y_{\mathrm{SRF}} =& 53.55 \times 10^{10} + 0.6283 \times 10^{10} X_1 - 0.8542 \times 10^{10} X_2 + 1.804 \times 10^{10} X_3 \\ & - 5.733 \times 10^{10} X_1 X_2 + 3.823 \times 10^{10} X_1 X_3 + 5.194 \times 10^{10} X_2 X_3 \\ & + 3.054 \times 10^{10} X_1^2 + 11.27 \times 10^{10} X_2^2 + 4.986 \times 10^{10} X_3^2 \end{aligned} \tag{2}$$

$$\begin{aligned} Y_{\mathrm{MC}} =& 76.31 - 0.0114 X_1 + 0.1113 X_2 + 0.243 X_3 - 0.441 X_1 X_2 + 0.2534 X_1 X_3 \\ & + 0.218 X_2 X_3 + 0.6346 X_1^2 + 1.11 X_2^2 + 0.6041 X_3^2 \end{aligned} \tag{3}$$

Meanwhile, the quadratic coefficient of the prediction model equation of sludge dewaterability is positive, so it is speculated that the quadratic surface model has an upward opening, that is, the regression equation has extreme points (Aziz *et al.* 2022). The existence of extreme points indicates that the sludge dewaterability has an optimal value. Through analysis of variance (ANOVA) and aboriginality test, the fitting regression model was analyzed and verified. The results are shown in Table S2 and Table S3.

The ANOVA of response value Y_{SRF} is shown in Table S2. Firstly, the *F*-test shows that the *F*-value of the SRF prediction model is 36.42, and the *P*-value is less than 0.0001, indicating that the prediction model is highly significant, only 0.01% of the probability will appear large *F*-value due to noise interference. For each model item, when the *P*-value is less than 0.05, it shows that the model item has good visibility (Ramachandra & Devatha 2020). In the first term of the SRF prediction model, the *P*-value of X_3 was <0.05, indicating that the influence of SBB dosage on SRF was more obvious. In the second term, the *P*-values of X_{12}, X_{22} and X_{32} were less than 0.05, indicating that X_{12}, X_{22} and X_{32} had significant effects on SRF. In the interaction term, the *P*-values of X_1X_2, X_1X_3 and X_2X_3 were less than 0.05, indicating that the interaction between each model item was more obvious. The lack of fit is used to describe the degree of difference between the test fitting and the regression model (Xiao *et al.* 2020). When the regression model can not fully explain the functional relationship between the response value and the influencing factors, it is shown as a mismatch. The *F*-value of the lack of fit of the SRF prediction

model is 0.8823, and the *P*-value is 0.5219, which indicates that the mismatch of the prediction model is not significant (*P*-value > 0.05), and the uncertainty error in the observation process will cause residual. The correlation coefficient (R^2) of the SRF prediction model is 0.9791, indicating that the model has a high degree of fit with the real situation. Meantime, the adjusted correlation coefficient (R^2_{adj}) of the SRF prediction model is 0.9522, indicating that only 5% of the variation response value of the model can not be accurately described (Aziz *et al.* 2022). In addition, the signal-to-noise ratio of the model is 16.1999. When the signal-to-noise ratio is greater than 4, the model is reasonable (Han *et al.* 2016). In response to surface optimization, the fitting degree of the regression model should be improved as much as possible to avoid bad results. Through the above analysis, the model equation (Equation (2)) has a good fitting degree to the experimental values. It is used to describe the relationship between the SRF response value and the three influencing factors of US cracking action time, CTS dosage and SBB dosage. The accuracy and authenticity are high, indicating that the experimental results have a good correlation with the prediction results provided by the model.

The ANOVA of the response value Y_{MC} is shown in Table S3. The *F*-value of the MC prediction model is 51.77, and the *P*-value is less than 0.0001, indicating that the model has strong aboriginality. In the first term of the MC prediction model, the *P*-value of X_3 was < 0.05, indicating that the SBB dosage had a greater impact on the MC of sludge cake MC. In the quadratic term, the *P*-values of X_{12}, X_{22} and X_{32} were less than 0.05, indicating that X_{12}, X_{22} and X_{32} had significant effects on MC. In the interaction terms, the *P*-values of X_1X_2, X_1X_3 and X_2X_3 were <0.05, indicating that the interaction between each model term was highly significant. The *F*-value of the lack of fit of the MC prediction model is 2.88, and the *P*-value is 0.1663, which indicates that the model mismatch is not significant (*P*-value > 0.05). The R^2 of the MC prediction model is 0.9852, and the R^2_{adj} is 0.9662, indicating that the MC change described by the prediction model is about 96%, and the model has high authenticity (Shi *et al.* 2015). Meanwhile, the signal-to-noise ratio of the MC prediction model is 19.5053, indicating that the model is reasonable. Moreover, further residual analysis of the model is carried out. The results are shown in text s1. In general, the model Equation (3) has a good fit, and the relationship between MC response value and US cracking action time, CTS dosage and SBB dosage is accurately described, and the experimental value is consistent with the predicted value.

3.3. Conditions for optimizing combined conditioning by RSM

3.3.1. Analysis of response surface and contour results

Using Design-Expert 12, the response variable regression equation is constructed into a three-dimensional surface map, which can intuitively see the interaction between various influencing factors and the influence on sludge dewaterability conditioning and obtain the optimal conditions for sludge dewatering. In addition, the contour map obtained by the projection of the response surface can also intuitively see that the point at the center of the circle is the extreme point, indicating that within the selected range of conditions, the response variable has the optimal value (Rashmi & Devatha 2022). Moreover, when the contour map is elliptical, the interaction between the selected two influencing factors is considered to be significant. When the contour shape tends to be circular, the interaction between the influencing factors is not obvious (Hu *et al.* 2019).

When the coding level of SBB is 0 (dosage is 0.5 g/g DS), the interaction between US cracking time and CTS dosage on SRF and MC is shown in Figure 1. Figure 1(a) shows that with the increase of US cracking time, sludge SRF gradually decreased, but with the increase of US action time, SRF began to rise; the influence of CTS on SRF was similar to that of US. With the increase in dosage, SRF decreased first and then increased. From Figure 1(a), the surface has a certain slope, indicating that US cracking time and CTS dosage and their interaction have a greater impact on sludge SRF; however, compared with the action time of US, the parabolic opening in the cross-section with CTS dosage as the horizontal axis is smaller, indicating that the CTS dosage has a greater impact on SRF. By analyzing the contour plot (Figure 1(b)), it can be found that the contour shape is elliptical, indicating that the interaction between US cracking time and CTS dosage has a strong impact on sludge SRF. Figure 1(c) is the effect of US cracking time and CTS dosage on MC. It can be found that with the increase in US cracking time and CTS dosage, MC first decreases and then increases. The response surface has a large slope, indicating that the US cracking time and CTS dosage and their interaction have a great influence on MC. Compared with the SRF response surface, the slope of the MC response surface is steeper, indicating that the US cracking time and CTS dosage and their interaction have a greater impact on MC. It can also be seen from the response surface diagram of MC that the opening degree of the cross-section parabola with US time as the horizontal axis is similar to that with CTS dosage as the horizontal axis, indicating that these two factors have a similar influence on MC. It can be seen from Figure 1(d) that the contour shape is elliptical, which again proves that the interaction between US cracking time and CTS dosage is obvious.

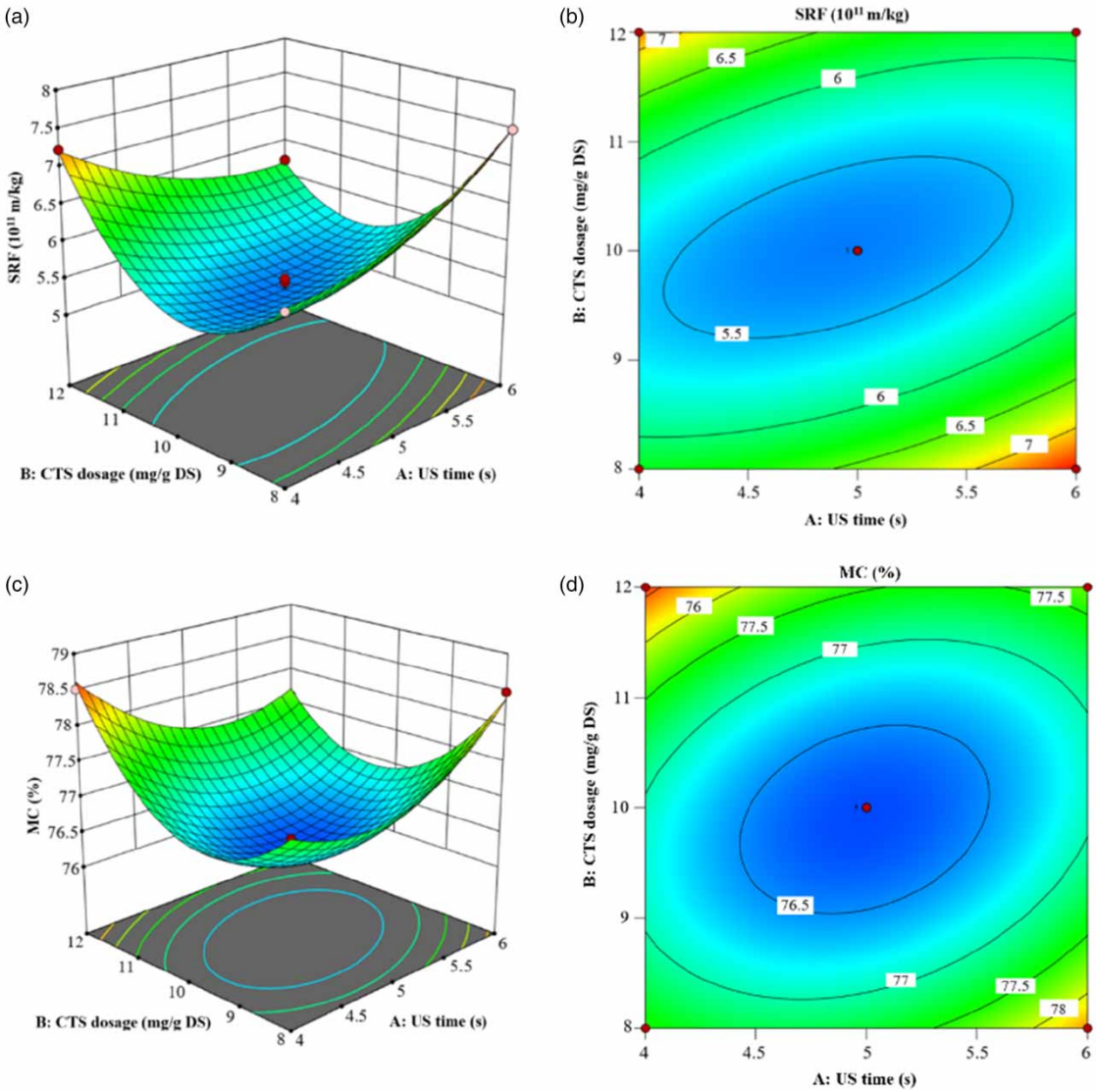

Figure 1 | Interaction of US cracking time and CTS dosage on SRF and MC. (a) 3d response surface plot of the effect of variables on SRF, (b) contour plot of the effect of variables on SRF, (c) 3d response surface plot of the effect of variables on MC, and (d) contour plot of the effect of variables on MC.

Moreover, the MC contour line (Figure 1(d)) is denser than the SRF contour line (Figure 1(b)), so it is considered that the interaction between the US crack time and the CTS dosage has a more obvious influence on MC.

When the CTS coding level is 0 (dosage is 10 mg/g DS), the interaction between US cracking time and SBB dosage on SRF and MC is shown in Figure 2. The figure shows that with the extension of US cracking time and the increase of SBB dosage, the SRF of sludge decreases first and then increases. Similarly, the MC also showed a decreasing trend with the extension of US cracking time and the increase of SBB dosage in a certain range. When it exceeded a certain range, MC would rebound. The response surface is relatively flat when the response variable is SRF, and the parabola opening in each section is large, which reflects that the influence of US cracking time and SBB dosage on sludge SRF is relatively small. Through the contour map of SRF, it is found that although the contour shape is elliptical, the density of the contour is small, which indicates that the interaction between US cracking time and SBB dosage is low. Compared with the response surface of SRF, the slope of the response surface of MC is steep, and the parabola opening in each section is small, indicating that the influence of US cracking time and SBB dosage on MC is relatively large. In addition, the line density of the MC contour map is larger

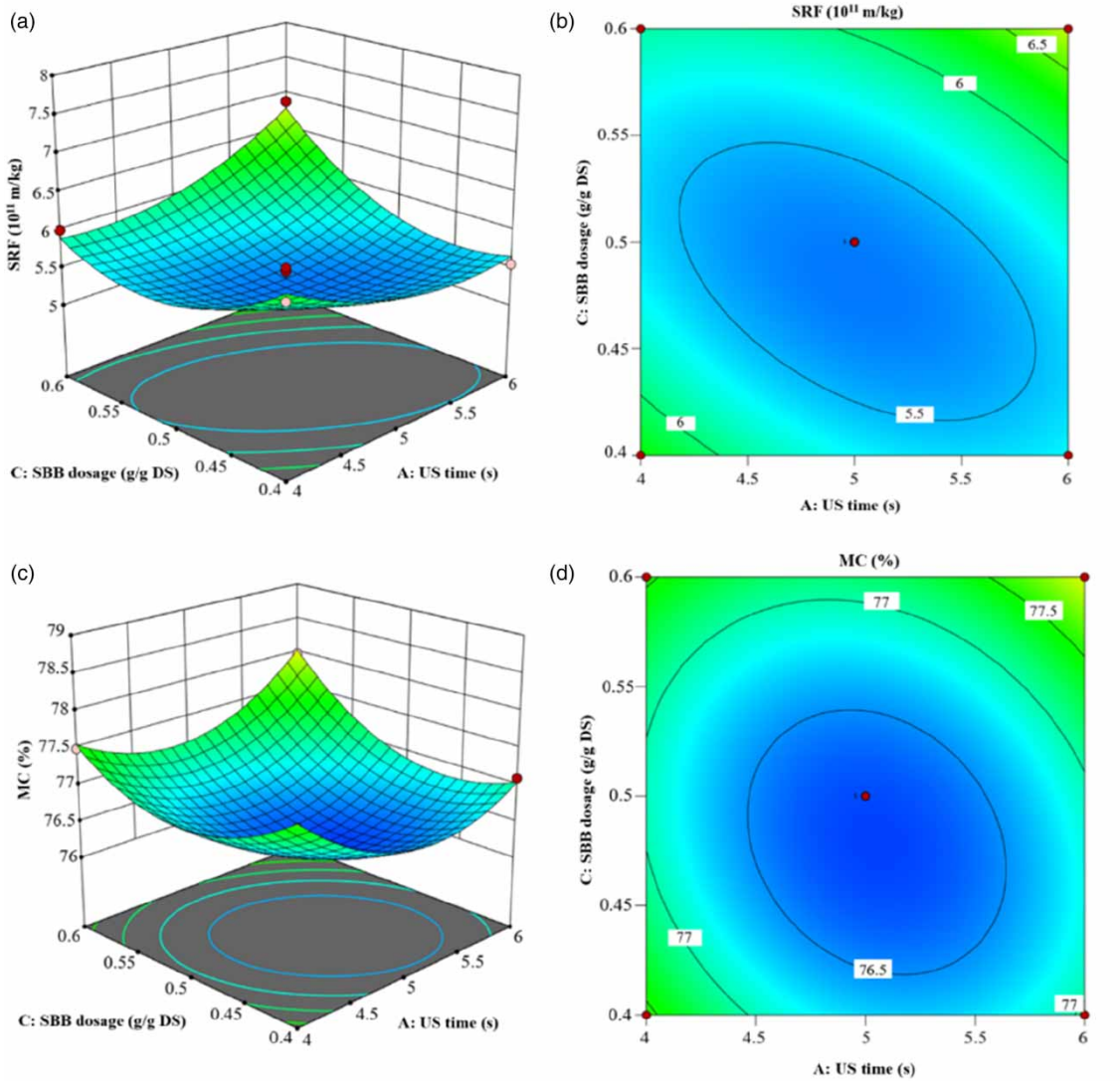

Figure 2 | Interaction of US cracking time and SBB dosage on SRF and MC. (a) 3d response surface plot of the effect of variables on SRF, (b) contour plot of the effect of variables on SRF, (c) 3d response surface plot of the effect of variables on MC, and (d) contour plot of the effect of variables on MC.

than that of the SRF contour map, which indicates that the interaction between US cracking time and SBB dosage on MC is more obvious.

When the encoding level of US is 0 (cracking time is 5 s), the interaction between CTS dosage and SBB dosage on SRF and MC is shown in Figure 3. The figure shows that with the increase of CTS and SBB dosage, sludge SRF first decreases and then increases. Similarly, MC also showed a decreasing trend in a certain range with the increase of CTS and SBB dosage. When CTS and SBB dosages were excessive, MC began to increase. By comparison, the slope bending degree of the SRF response surface was similar to that of the MC response surface, which was relatively steep, indicating that CTS, SBB and their dosage had great influence on sludge dewaterability. In addition, the line density of the SRF contour map and MC contour map is larger, which reflects the interaction between CTS and SBB on sludge dewaterability.

Based on the above analysis, the interaction between US cracking time and CTS dosage, the interaction between US cracking time and SBB dosage and the interaction between CTS dosage and SBB dosage all affected the sludge dewatering performance, which was consistent with the variance analysis of the interaction items (X_1X_2, X_1X_3, X_2X_3) in the above

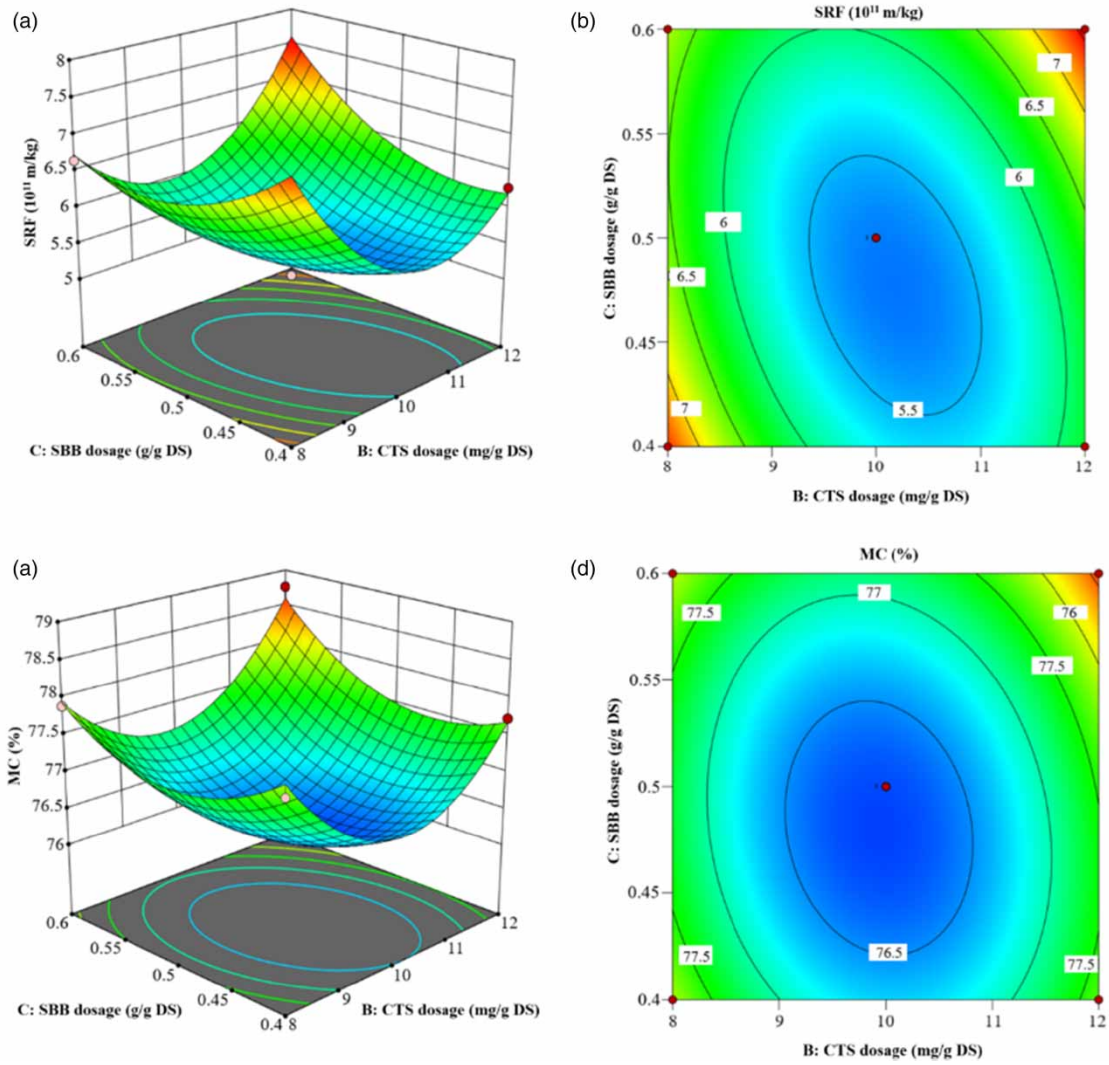

Figure 3 | Interaction between CTS dosage and SBB dosage on SRF and MC. (a) 3d response surface plot of the effect of variables on SRF, (b) contour plot of the effect of variables on SRF, (c) 3d response surface plot of the effect of variables on MC, and (d) contour plot of the effect of variables on MC.

model. At the same time, it was well confirmed that there was a synergistic effect between US cracking, CTS flocculation and SBB skeleton adsorption on sludge dewaterability. However, according to the analysis of the response surface and contour map, the influence degree of each interaction on sludge dewaterability is different and the order of its influence is $X_2X_3 > X_1X_2 > X_1X_3$. It is inferred that CTS and SBB contribute more to the process of US + CTS + SBB combined strengthening sludge dewatering.

3.3.2. Condition optimization and model verification

Design-Expert 12 software was used to optimize the conditions of US time, CTS dosage and SBB dosage in US + CTS + SBB conditioning. According to the minimum principle of SRF, the first optimization result was obtained: US cracking time was 5.0818 s, CTS dosage was 10.1104 mg/g DS, and SBB dosage was 0.4765 g/g DS. At this time, the SRF predicted by the model was 5.3296×10^{11} m/kg, and the MC was 76.294%. According to the minimum principle of MC, the second optimization results were obtained: US cracking time was 5.0750 s, CTS dosage was 10.1001 mg/g DS, SBB dosage was 0.4774 g/g DS. At this time, the SRF predicted by the model was 5.3304×10^{11} m/kg, and the MC was 76.2931%. The desirability values of the two optimization results are 0.91, approaching 1, indicating that the reliability of the optimization results is extremely

high. By comparing the two optimization results, it can be found that the obtained condition parameters are very close. Combined with the difficulty of controlling the condition parameters in the actual conditioning process, the optimization conditions are corrected. The modified conditioning conditions are: US cracking time is 5.08 s, CTS dosage is 10.1 mg/g DS and SBB dosage is 0.477 g/g DS.

In order to verify the accuracy and reliability of the theoretical optimization value obtained by the model, three repeated tests were carried out according to the above-optimized conditioning conditions. The average results are as follows: SRF is 5.4125×10^{11} m/kg, MC is 76.8123% and the relative error is small. It proves that the RSM model can effectively and reasonably optimize the condition parameters of the sludge dewatering process, which has a certain reference value for practical engineering applications.

3.4. Effects of optimized process on sludge properties and the conjecture of conditioning mechanism

In this study, the EPS and surface functional groups before and after sludge conditioning were characterized and analyzed, and the effects of the optimized combined process on the dewatering performance of sludge were discussed. Figure 4(a) shows the EPS content of each layer in the sludge (the specific EPS component data are shown in Table S4). The results showed that after optimizing the process conditions, the contents of PN and PS in each layer of EPS decreased to varying degrees, indicating that the content of PN and PS in EPS is positively related to the sludge dewaterability. Among them, the decline of PN content is large, and PN is widely reported as the main water-holding organic matter affecting sludge dehydration (Wu *et al.* 2017; Zhu *et al.* 2020; Yu *et al.* 2021). Certainly, PS is also one of the sources of sludge hydrophilicity and viscosity (Cao *et al.* 2021), and the decrease in its content will also promote the improvement of sludge dewaterability. In the combined conditioning process, US will destroy the EPS structure, promote the transfer of PN and PS from the inner EPS to the outer layer (Chen *et al.* 2017; Huang *et al.* 2020a, 2020b), and finally release them into S-EPS or sludge liquid phase. CTS may also squeeze the EPS structure by compressing the electric double layer, and the release promotes the migration of PN and PS. Then SBB can adsorb PN and PS in S-EPS and promote the dissolution of inner EPS (Yang *et al.* 2022a). Therefore, the water-holding capacity of the sludge is reduced.

The dewatering performance of sludge is closely related to the functional groups on the sludge surface. In order to further understand the influence of the optimized process on the sludge properties, FTIR is used to monitor the functional groups on the conditioned sludge surface. The results are shown in Figure 4(b). The results showed that the characteristic peaks appeared at 3,419, 2,927, 1,653, 1,537, 1,411 and 1,041 cm^{-1} of the raw sludge samples. The peaks near 3,419 cm^{-1} correspond to the stretching vibration of O–H, and the peaks near 2,927 and 2,862 cm^{-1} are related to the symmetric and asymmetric stretching vibration of CH_2 in lipids. The peak near 1,653 cm^{-1} indicates the stretching vibration of C = O and C–N in the PN amide I band. Moreover, the peak near 1,537 cm^{-1} implies the stretching vibration of N–H and C–N

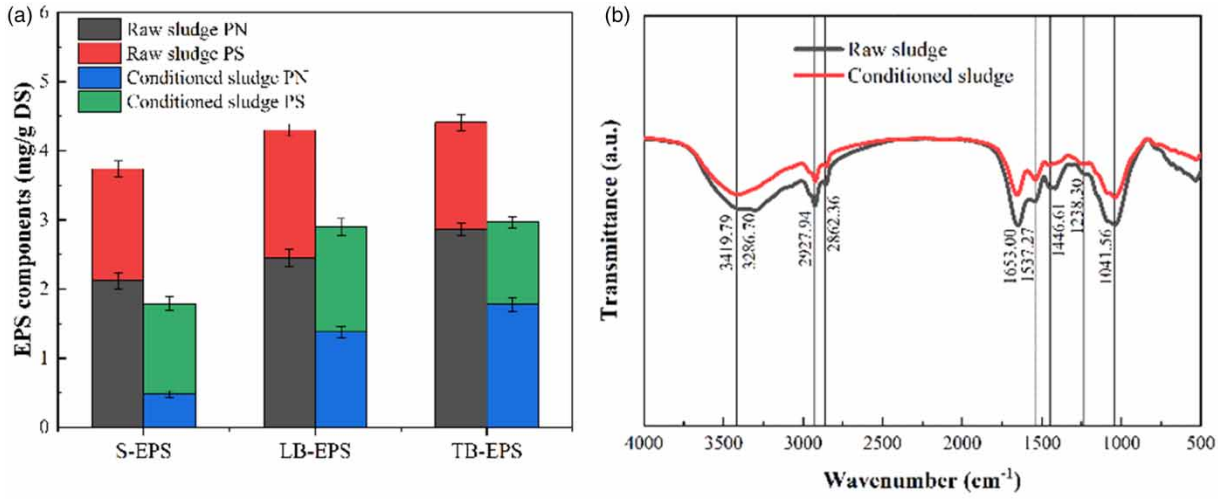

Figure 4 | Effect of conditioning on sludge EPS components (a) and surface functional groups (b).

at CO-NH in the PN amide II band. The peak near 1,411cm^{-1} represents the symmetric stretching vibration of C–O in carboxylate. The peak near 1,041 cm^{-1} represents the stretching vibration of C–O in PS. It can be seen that the organic matter in the sludge is mainly composed of hydrocarbons, PN and PS (Badireddy *et al.* 2010). After the optimized process conditioning, the protein-related absorption peaks (C = O, C–H, C–N) in the spectrum are weakened, which indicates that the combined process can effectively reduce the PN content in the sludge, thereby reducing the hydrophilic groups in the sludge, thereby enhancing the sludge dewaterability (Zhang *et al.* 2020).

From a statistical point of view, US, CTS and SBB show synergy in the process of combined conditioning. Compared to the addition and conditioning of CTS and SBB, the use of US conditioning alone has a relatively small improvement in the overall dewaterability of sludge. But according to our research findings, the cavitation effect of US can fully decompose the sludge flocs and surface EPS structure, convert a large amount of bound water into free water and release some intracellular substances and negatively charged groups, which can provide more binding sites for the subsequent addition of CTS. In addition, US can also dissolve the water-holding substances on EPS, promoting their adsorption on SBB. it was found that the US step is irreplaceable, and the change in sludge properties by US lays the foundation for subsequent conditioning, with a synergistic effect with CTS and SBB. Combined with the changes in sludge properties, the following assumptions were made : First, the sludge was decomposed by the cavitation action of US, and the structure of sludge bacterial micelles and EPS were disintegrated, and part of the bound water was released, so that the water-holding substances on EPS were dissolved, and its adsorption on SBB was promoted. Secondly, CTS makes small sludge particles form large floc structure again, reduces the specific surface area of floc and strengthens the solid–liquid separation ability. Finally, SBB adsorbed the water-holding substances in S-EPS, promoted the dissolution of LB-EPS and TB-EPS, exposed more internal hydrophobic groups to improve the hydrophobic expression and weakened the polarity between the floc and water molecules. Thus, sludge dewatering performance is improved.

3.5. Sludge incineration disposal analysis

3.5.1. Heat value analysis of sludge cake

In order to explore the effect of conditioning methods on the calorific value of sludge cake, the low calorific value of sludge cake before and after conditioning was measured by an oxygen bomb calorimeter. The results are shown in Table 3. The heat value of untreated raw mud cake is 10,523 kJ/kg, which is similar to that of low-grade coal. When the combustion heat value of sludge is greater than 6,000 kJ/kg, it is considered that sludge can generate electricity or heat continuously and stably (Chen *et al.* 2012). The calorific value of sludge cake treated by SBB alone was 12,125 kJ/kg, which was 16.82% higher than that of untreated sludge. The calorific value of sludge cake treated by US + CTS + SBB was 12,378 kJ/kg, which was 16.96% higher than that of untreated sludge. It can be found that the heat value of mud cake after US + CTS + SBB combined conditioning is slightly higher than that of mud cake after SBB alone conditioning, but the difference is small, which may be because CTS as an organic flocculant is helpful to improve the heat value (Li *et al.* 2022). However, the fundamental reason is that the increase in calorific value is attributed to SBB, which is a kind of carbon material. The incorporation of sludge improves the carbon fixation of sludge cake and plays a role in combustion (Cao *et al.* 2019). By measuring the combustion calorific value of SBB material alone, it was found that the calorific value was as high as 13,374 kJ/kg, indicating that SBB material itself had a high calorific value, which confirmed that it had made a significant contribution to the improvement of calorific value when it was combined with sludge cake.

3.5.2. Thermo gravimetric analysis of sludge cake

In order to explore the state change of sludge cake during combustion, thermogravimetric analysis (TG-DTG) of sludge cake was carried out by synchronous thermal analyzer. The test results are shown in Figure 5. The TG curve is expressed

Table 3 | Calorific value of sludge cake

Category	Raw sludge cake	SBB[a]-processed sludge cake	US[b] + CTS[c] + SBB conditioning sludge cake	SBB material
Calorific value (kJ/kg)	10,523	12,125	12,308	13,374

[a]Sludge-based biochar.
[b]Ultrasonic.
[c]Chitosan.

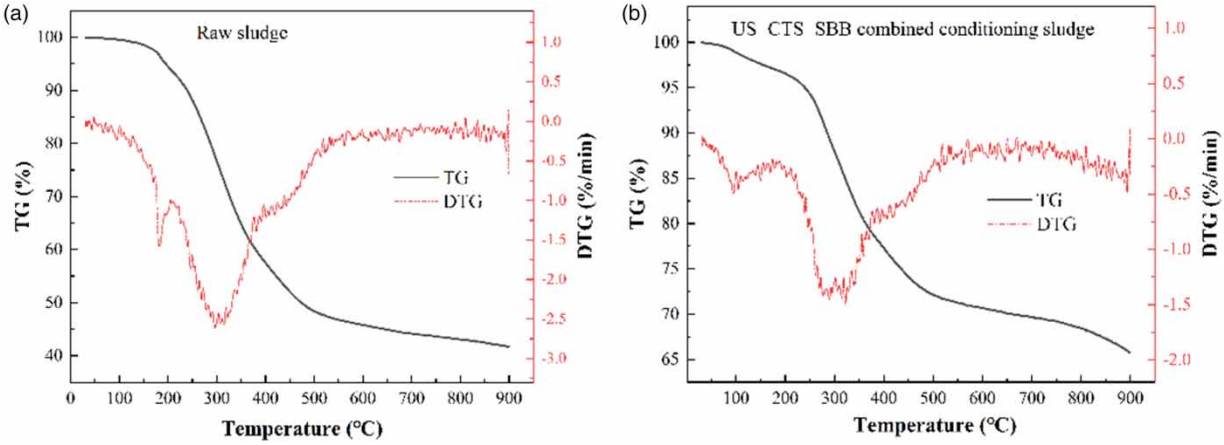

Figure 5 | TG and DTG curves of the cake of (a) raw sludge and (b) US + CTS + SBB combined conditioning sludge. TG, thermogravimetric; DTG, derivative thermogravimetry.

as the weight loss change of the sample at the set heating rate. The DTG curve is obtained by the first-order differential of the TG curve to temperature or time, indicating the relationship between the weight change of the sample and the temperature or time. When the weight change of the sample is very small, the steps on the TG curve are not easy to identify and can be distinguished by the DTG curve (Mo *et al.* 2021). It can be seen from Figure 4(a) that there are two weight loss peaks in the DTG curve of the raw sludge, and the first weight loss peak is obvious. From the first weight loss step on the TG curve, it can be seen that the temperature at which it begins to lose weight is 111 °C and reaches the weight loss peak at 182 °C, with the weight loss rate of 6.85%. This is mainly because when the ambient temperature reaches 111 °C, the remaining bound water in the mud cake begins to evaporate and reduce weight; when the temperature reaches 182 °C, the moisture in the mud cake sample is basically removed. For the sludge cake after combined conditioning, there was an obvious weight loss step on the TG curve, and the first weight loss peak appeared on the DTG curve. The temperature at the beginning of the weight loss was 72 °C, and the temperature at the time of reaching the weight loss peak was 104 °C. The weight loss rate was 2.75%, indicating that the moisture in the sludge cake was almost removed at 104 °C (Wu *et al.* 2020b). Compared with untreated raw sludge, the occurrence of weightlessness peak is much earlier, which is first because the bound water content in the sludge after combined conditioning is less, which can also be obtained according to the difference in weightlessness rate (Cao *et al.* 2019). Secondly, the binding energy between water molecules and the solid phase in the sludge after combined conditioning was greatly weakened, so that these binding bonds could be broken at low temperatures, so that the residual water in the sludge cake could be evaporated more quickly (Menon *et al.* 2020). Meantime, this also shows that the mud cake added with SBB material has a lower ignition temperature, which is an important parameter of fuel.

The TG curve of the second weightlessness peak of the raw sludge and the combined conditioning sludge was not obvious. The temperature of the second weightlessness peak of the raw sludge cake was 295 °C, and the temperature of the second weightlessness peak of the combined conditioning sludge cake was 289 °C. The second weightlessness peak was mainly due to the combustion of volatile substances in the sludge cake (Zhai *et al.* 2012). Meantime, it can be found that a small weight loss peak appears after the second weight loss peak of the prepared cake. It is speculated that the weight loss peak is not obvious because the volatiles in SBB begin to burn, while the volatiles in SBB are less. In addition, from 530 to 900 °C, the weight loss curve of the original mud cake was basically stable, indicating that the combustion termination temperature of the mud cake was 530 °C, and the final weight loss rate was 51.44%. The weight loss curve of the combined conditioning mud cake was stable from 530 to 735 °C, but it began to decline after 735 °C. The weight loss rate at 900 °C was 31.44%, indicating that there were still combustible substances in the mud cake, and the burnout temperature was much higher than that of the original mud cake. According to previous studies (Yang *et al.* 2022a), SBB has high carbon content and oxygen content. Carbon element is the main element for heat generation in the combustion process, and oxygen is the combustion-supporting element. Therefore, the incorporation of SBB into sludge can improve the carbon content of sludge cake and make it more flammable.

3.6. Process prospect and limitations

Although the US + CTS + SBB process seems to use more processing units, it has strong wide applicability. Because this process does not need to overturn and rebuild the existing sludge treatment facilities of the WWTPs, it only needs to be reconstructed on the original basis, which can greatly reduce the investment of funds. Firstly, the US cracking step only needs to be carried out on the sludge conveying pipeline in front of the sludge regulating tank. A section of pipeline with US equipment is set up to control the residence time of sludge in the ultrasonic area by controlling the flow. The residence time is the US cracking time. Secondly, the original dosing equipment shall be modified, and CTS and SBB shall be added to the sludge regulating tank in sections, and a sludge buffer tank shall be set in front of the mechanical dewatering equipment to ensure that CTS and SBB can fully react with the sludge, so as to change the dewatering property of the sludge. When the WWTP has no follow-up disposal facilities, it can save part of the cost of sludge transportation. The increase in sludge cake heat value will also bring economic benefits to the WWTP. Therefore, this process has great application prospects. This study also has some limitations. For instance, while the addition of SBB can effectively improve sludge dewatering performance, the addition of skeleton particles increases the dry weight of sludge, which may offset some of the water reduction effects reflected in the improved dewatering performance. Additionally, the use of zinc chloride as a pre-activator may increase the zinc ion content in the sludge cake, which may make the dehydrated sludge more suitable for incineration disposal and not suitable for land use.

4. CONCLUSION

In order to improve the sludge dewatering performance, this study optimized the dewatering performance of US + CTS + SBB combined process by using the RSM and BBD methods. The SRF prediction model and MC prediction model were constructed based on the experimental results. According to the ANOVA and 3D surface graphs, the effect of SBB dosage on sludge dewaterability is more obvious, and the interaction between CTS dosage and SBB dosage is the most significant in the interaction term. Combined with the optimization results and actual production, the optimal conditions of US + CTS + SBB combined conditioning process are as follows: US cracking time is 5.08 s, CTS dosage is 10.1 mg/g DS, and SBB dosage is 0.477 g/g DS. Under this condition, the SRF is 5.4125×10^{11} m/kg, and MC is 76.8123%. The tests confirmed that the actual values of SRF and MC were generally in agreement with the predicted values. In addition, the calorific value of the sludge cake treated by US + CTS + SBB was increased by 16.96% compared with the untreated sludge. The burnout temperature of the combined conditioned sludge cake is much higher than that of the original sludge cake, and the combustion is more durable. This is because the mixing of SBB with sludge increases the carbon fixation of the sludge cake and plays a role in combustion. The results of the thermogravimetric analysis showed that the combined conditioned sludge contained less bound water, and the bond energy between water molecules and the solid phase was greatly weakened.

ACKNOWLEDGEMENTS

This research was supported by the Natural Science Foundation of Gansu Province (22JR5RA254), the Outstanding Postgraduate Innovation Star Project of Gansu Provincial Department Education (2023CXZX- 461), Wenzhou Basic Social Development Science and Technology Project of China (S20220010) and the National Natural Science Foundation of China (22066012).

DATA AVAILABILITY STATEMENT

All relevant data are included in the paper or its Supplementary Information.

CONFLICT OF INTEREST

The authors declare there is no conflict.

REFERENCES

Agarwal, S., Abu-Orf, M. & Novak, J. T. 2005 Sequential polymer dosing for effective dewatering of ATAD sludges. *Water Research* **39** (7), 1301–1310.

Aziz, K., Aziz, F., Mamouni, R., Aziz, L. & Saffaj, N. 2022 Engineering of highly *Brachychiton populneus* shells@polyaniline bio-sorbent for efficient removal of pesticides from wastewater: Optimization using BBD-RSM approach. *Journal of Molecular Liquids* **346**, 117092.

Badireddy, A. R., Chellam, S., Gassman, P. L., Engelhard, M. H., Lea, A. S. & Rosso, K. M. 2010 Role of extracellular polymeric substances in bioflocculation of activated sludge microorganisms under glucose-controlled conditions. *Water Research* **44** (15), 4505–4516.

Bala Subramanian, S., Yan, S., Tyagi, R. D. & Surampalli, R. Y. 2010 Extracellular polymeric substances (EPS) producing bacterial strains of municipal wastewater sludge: Isolation, molecular identification, EPS characterization and performance for sludge settling and dewatering. *Water Research* **44** (7), 2253–2266.

Cao, B., Wang, R., Zhang, W., Wu, H. & Wang, D. 2019 Carbon-based materials reinforced waste activated sludge electro-dewatering for synchronous fuel treatment. *Water Research* **149**, 533–542.

Cao, B., Zhang, T., Zhang, W. & Wang, D. 2021 Enhanced technology based for sewage sludge deep dewatering: A critical review. *Water Research* **189**, 116650.

Chen, C., Zhang, P., Zeng, G., Deng, J., Zhou, Y. & Lu, H. 2010 Sewage sludge conditioning with coal fly ash modified by sulfuric acid. *Chemical Engineering Journal* **158** (3), 616–622.

Chen, W. S., Lin, C. W., Chang, F.-C., Lee, W.-J. & Wu, J.-L. 2012 Utilization of spent activated carbon to enhance the combustion efficiency of organic sludge derived fuel. *Bioresource Technology* **113**, 73–77.

Chen, Z., Zhang, W., Wang, D., Ma, T. & Bai, R. 2015 Enhancement of activated sludge dewatering performance by combined composite enzymatic lysis and chemical re-flocculation with inorganic coagulants: Kinetics of enzymatic reaction and re-flocculation morphology. *Water Research* **83**, 367–376.

Chen, W., Gao, X., Xu, H., Cai, Y. & Cui, J. 2017 Influence of extracellular polymeric substances (EPS) treated by combined ultrasound pretreatment and chemical re-flocculation on water treatment sludge settling performance. *Chemosphere* **170**, 196–206.

Ducoli, S., Zacco, A. & Bontempi, E. 2021 Incineration of sewage sludge and recovery of residue ash as building material: A valuable option as a consequence of the COVID-19 pandemic. *Journal of Environmental Management* **282**, 111966.

Fan, X., Wang, Y., Zhang, D., Guo, Y., Gao, S., Li, E. & Zheng, H. 2021 Corrigendum to 'Effects of acid, acid-ZVI/PMS, Fe(II)/PMS and ZVI/PMS conditioning on the wastewater activated sludge (WAS) dewaterability and extracellular polymeric substances (EPS)' [J. Environ. Sci. 91 (2020) 73–84]. *Journal of Environmental Sciences (China)* **99**, 274–274.

Feng, G., Tan, W., Zhong, N. & Liu, L. 2014 Effects of thermal treatment on physical and expression dewatering characteristics of municipal sludge. *Chemical Engineering Journal* **247**, 223–230.

Ferreira, S. L. C., Bruns, R. E., Ferreira, H. S., Matos, G. D., David, J. M., Brandão, G. C., da Silva, E. G. P., Portugal, L. A., dos Reis, P. S., Souza, A. S. & dos Santos, W. N. L. 2007 Box-Behnken design: An alternative for the optimization of analytical methods. *Analytica Chimica Acta* **597** (2), 179–186.

Gao, W. 2011 Freezing as a combined wastewater sludge pretreatment and conditioning method. *Desalination* **268** (1), 170–173.

Ge, D., Yuan, H., Shen, Y., Zhang, W. & Zhu, N. 2019 Improved sludge dewaterability by tannic acid conditioning: Temperature, thermodynamics and mechanism studies. *Chemosphere* **230**, 14–23.

Ge, D., Bian, C., Yuan, H. & Zhu, N. 2020 An in-depth study on the deep-dewatering mechanism of waste activated sludge by ozonation pre-oxidation and chitosan re-flocculation conditioning. *Science of The Total Environment* **714**, 136627.

Guo, J. & Chen, C. 2017 Sludge conditioning using the composite of a bioflocculant and PAC for enhancement in dewaterability. *Chemosphere* **185**, 277–283.

Han, Y., Zhou, M., Wan, S., Xue, F., Liang, A., Yuan, J. & Hou, H. 2016 Optimization of sludge dewatering process by inorganic conditioners under mild thermal treatment. *Desalination and Water Treatment* **57** (59), 28661–28669.

Hu, D., Zhang, Y. & Zhang, C. 2019 Effects of EDTA on phosphorus release in excess sludge and phosphorus recovery by MAP. *China Environmental Science* **39** (4), 1611–1618.

Huang, J., Liang, J., Yang, X., Zhou, J., Liao, X., Li, S., Zheng, L. & Sun, S. 2020a Ultrasonic coupled bioleaching pretreatment for enhancing sewage sludge dewatering: Simultaneously mitigating antibiotic resistant genes and changing microbial communities. *Ecotoxicology and Environmental Safety* **193**, 110349.

Huang, K., Chen, J., Mengxin, G., Hui, X. & Li, L. 2020b Effects of biochars on the fate of antibiotics and their resistance genes during vermicomposting of dewatered sludge. *Journal of Hazardous Materials* **397**, 122767.

Li, A., Huang, C., Feng, X., Li, Y., Yang, H., Wang, S. & Li, J. 2022 Upgradation of sludge deep dewatering conditioners through persulfate activated by ferrous: Compatibility with sludge incineration, dewatering mechanism, ecological risks elimination and carbon emission performance. *Environmental Research* **211**, 113024.

Liang, S., Yang, L., Chen, H., Yu, W., Tao, S., Yuan, S., Xiao, K., Hu, J., Hou, H., Liu, B. & Yang, J. 2021 Phosphorus recovery from incinerated sewage sludge ash (ISSA) and reutilization of residues for sludge pretreated by different conditioners. *Resources, Conservation and Recycling* **169**, 105524.

Lin, W., Liu, X., Ding, A., Ngo, H. H., Zhang, R., Nan, J., Ma, J. & Li, G. 2022 Advanced oxidation processes (AOPs)-based sludge conditioning for enhanced sludge dewatering and micropollutants removal: A critical review. *Journal of Water Process Engineering* **45**, 102468.

Lu, M. C., Lin, C. J., Liao, C. H., Ting, W. P. & Huang, R. Y. 2001 Influence of pH on the dewatering of activated sludge by Fenton's reagent. *Water Science and Technology* **44**, 327–332.

Masihi, H. & Badalians Gholikandi, G. 2021 Using thermal-acidic-modified kaolin as a physical-chemical conditioner for waste activated sludge dewatering. *Chemical Engineering Journal* **412**, 128664.

Menon, U., Suresh, N., George, G., Ealias, A. M. & Saravanakumar, M. P. 2020 A study on combined effect of Fenton and free nitrous acid treatment on sludge dewaterability with ultrasonic assistance: Preliminary investigation on improved calorific value. *Chemical Engineering Journal* **382**, 123035.

Mo, W., Wu, Z., He, X., Qiang, W., Wei, B., Wei, X., Wu, Y., Fan, X. & Ma, F. 2021 Functional group characteristics and pyrolysis/combustion performance of fly ashes from Karamay oily sludge based on FT-IR and TG-DTG analyses. *Fuel* **296**, 120669.

Mohajeri, S., Aziz, H. A., Isa, M. H., Zahed, M. A. & Adlan, M. N. 2010 Statistical optimization of process parameters for landfill leachate treatment using electro-Fenton technique. *Journal of Hazardous Materials* **176** (1), 749–758.

Mowla, D., Tran, H. N. & Allen, D. G. 2013 A review of the properties of biosludge and its relevance to enhanced dewatering processes. *Biomass and Bioenergy* **58**, 365–378.

Qi, Y., Thapa, K. B. & Hoadley, A. F. 2011 Application of filtration aids for improving sludge dewatering properties – A review. *Chemical Engineering Journal* **171** (2), 373–384.

Ramachandra, R. H. & Devatha, C. P. 2020 Experimental investigation on sludge dewatering using granulated blast furnace slag as skeleton material. *Environmental Science and Pollution Research* **27** (11), 11870–11881.

Rashmi, H. R. & Devatha, C. P. 2022 Dewatering performance of sludge using coconut shell biochar modified with ferric chloride (sludge dewatering using bio-waste). *International Journal of Environmental Science and Technology* **19** (7), 6033–6044.

Shi, L., Wei, D., Ngo, H. H., Guo, W., Du, B. & Wei, Q. 2015 Application of anaerobic granular sludge for competitive biosorption of methylene blue and Pb(II): Fluorescence and response surface methodology. *Bioresource Technology* **194**, 297–304.

Shi, C., Sun, W., Sun, Y., Chen, L., Xu, Y. & Tang, M. 2019 Synthesis, characterization, and sludge dewaterability evaluation of the chitosan-based flocculant CCPAD. *Polymers* **11**, 95.

Velghe, I., Carleer, R., Yperman, J., Schreurs, S. & D'Haen, J. 2012 Characterisation of adsorbents prepared by pyrolysis of sludge and sludge/disposal filter cake mix. *Water Research* **46** (8), 2783–2794.

Wang, J., Liu, H., Deng, H., Jin, M., Xiao, H. & Yao, H. 2020 Deep dewatering of sewage sludge and simultaneous preparation of derived fuel via carbonaceous skeleton-aided thermal hydrolysis. *Chemical Engineering Journal* **402**, 126255.

Wong, J. W. C., Zhou, J., Kurade, M. B. & Murugesan, K. 2015 Influence of ferrous ions on extracellular polymeric substances content and sludge dewaterability during bioleaching. *Bioresource Technology* **179**, 78–83.

Wu, B., Su, L., Song, L., Dai, X. & Chai, X. 2017 Exploring the potential of iTRAQ proteomics for tracking the transformation of extracellular proteins from enzyme-disintegrated waste activated sludge. *Bioresource Technology* **225**, 75–83.

Wu, B., Dai, X. & Chai, X. 2020a Critical review on dewatering of sewage sludge: Influential mechanism, conditioning technologies and implications to sludge re-utilizations. *Water Research* **180**, 115912.

Wu, J., Lu, T., Yang, G., Meng, W. & Chen, Y. 2020b Self-recycling of sewage sludge as a coagulant and mechanism in sewage sludge dewatering. *Journal of Material Cycles and Waste Management* **22** (6), 1–10.

Xiao, J., Ge, D., Yuan, H. & Zhu, N. 2020 Waste activated sludge conditioning in a new Fe^{2+}/persulfate/tannic acid process: Effectiveness and optimization study to enhance dewaterability. *Journal of Environmental Chemical Engineering* **8** (3), 103785.

Xu, X., Cao, D., Wang, Z., Liu, J., Gao, J., Sanchuan, M. & Wang, Z. 2019 Study on ultrasonic treatment for municipal sludge. *Ultrasonics Sonochemistry* **57**, 29–37.

Yang, Y., Yang, X., Wang, X., Yang, Q., Xu, W. & Li, Y. 2022a Explore the closed-loop disposal route of surplus sludge: Sludge self-circulation preparation of sludge-based biochar (SBB) to enhance sludge dewaterability. *Colloids and Surfaces A: Physicochemical and Engineering Aspects* **638**, 128304.

Yang, Y., Yang, X., Yang, Q., Zhang, H., Xu, W., Zhu, L., Ma, P. & Li, Y. 2022b Exploring the feasibility and potential mechanism of synergistic enhancement of sludge dewaterability by ultrasonic cracking, chitosan re-flocculation and sludge-based biochar adsorption of water-holding substances. *Journal of Environmental Chemical Engineering* **10** (5), 108303.

Yu, G.-H., He, P.-J., Shao, L.-M. & Zhu, Y.-S. 2008 Extracellular proteins, polysaccharides and enzymes impact on sludge aerobic digestion after ultrasonic pretreatment. *Water Research* **42** (8), 1925–1934.

Yu, W., Wen, Q., Yang, J., Xiao, K., Zhu, Y., Tao, S., Liang, S., Hu, S., Wu, Q., Hou, H., Liu, B. & Hu, J. 2021 Novel insights into extracellular polymeric substance degradation, hydrophilic/hydrophobic characteristics, and dewaterability of waste activated sludge pretreated by hydroxylamine enhanced fenton oxidation. *ACS ES&T Engineering* **1** (3), 385–392.

Zhai, Y., Peng, W., Zeng, G., Fu, Z., Lan, Y., Chen, H., Wang, C. & Fan, X. 2012 Pyrolysis characteristics and kinetics of sewage sludge for different sizes and heating rates. *Journal of Thermal Analysis and Calorimetry* **107** (3), 1015–1022.

Zhang, W., Peng, S., Xiao, P., He, J., Yang, P., Xu, S. & Wang, D. 2015 Understanding the evolution of stratified extracellular polymeric substances in full-scale activated sludges in relation to dewaterability. *RSC Advances* **5** (2), 1282–1294.

Zhang, X., Cai, H., Shen, J. & Zhang, H. 2018 Effects of potassium permanganate conditioning on dewatering and rheological behavior of pulping activated sludge: Mechanism and feasibility. *RSC Advances* **8**, 41172–41180.

Zhang, J., Hu, Q., Lu, J. & Lin, S. 2019 Study on the effect of chitosan conditioning on sludge dewatering. *Water Science and Technology* **79** (3), 501–509.

Zhang, W., Dai, X., Dong, B. & Dai, L. 2020 New insights into the effect of sludge proteins on the hydrophilic/hydrophobic properties that improve sludge dewaterability during anaerobic digestion. *Water Research* **173**, 115503.

Zhou, X., Jiang, G., Wang, Q. & Yuan, Z. 2014 A review on sludge conditioning by sludge pre-treatment with a focus on advanced oxidation. *RSC Advances* **4** (92), 50644–50652.

Zhu, Y. w., Xiao, K. k., Zhou, Y., Yu, W., Tao, S., Le, C., Lu, D., Yu, Z., Liang, S., Hu, J., Hou, H., Liu, B. & Yang, J. 2020 Profiling of amino acids and their interactions with proteinaceous compounds for sewage sludge dewatering by Fenton oxidation treatment. *Water Research* **175**, 115645.

Zielewicz, E. 2016 Effects of ultrasonic disintegration of excess sewage sludge. *Topics in Current Chemistry* **374** (5), 67.

Zolgharnein, J., Shahmoradi, A. & Ghasemi, J. B. 2013 Comparative study of Box–Behnken, central composite, and Doehlert matrix for multivariate optimization of Pb (II) adsorption onto Robinia tree leaves. *Journal of Chemometrics* **27** (1–2), 12–20.

First received 8 August 2023; accepted in revised form 20 February 2024. Available online 13 March 2024